Mechanism of Zn stabilization in hydroxyapatite and hydrated (0 0 1) surfaces of hydroxyapatite

2010 J. Phys.: Condens. Matter 22 145502

(http://iopscience.iop.org/0953-8984/22/14/145502)

J. Phys.: Condens. Matter **22** (2010) 145502 (7pp) doi:10.1088/0953-8984/22/14/145502

Mechanism of Zn stabilization in hydroxyapatite and hydrated (0 0 1) surfaces of hydroxyapatite

M Matos[1], J Terra[2] and D E Ellis[3]

[1] Departamento de Física, PUC-Rio, Gávea, CEP 22453-900, Caixa Postal 38071, Rio de Janeiro, RJ, Brazil
[2] Centro Brasileiro de Pesquisas Físicas, Rua Xavier Sigaud 150, Rio de Janeiro 22290-180, RJ, Brazil
[3] Department of Chemistry and Materials Research Center, Northwestern University, Evanston, IL 60208, USA

E-mail: maria.matos@fis.puc-rio.br

Received 15 December 2009, in final form 2 February 2010
Published 23 March 2010
Online at stacks.iop.org/JPhysCM/22/145502

Abstract

A basic understanding of Zn incorporation on bulk and hydrated (0 0 1) surfaces of hydroxyapatite (HA) is attained through electronic structure calculations which use a combined first principles density functional (DFT) and extended Hückel tight binding (EHTB) methodology. A Zn substituted hydroxyapatite relaxed structure is obtained through a periodic cell DFT geometry optimization method. Electronic structure properties are calculated by using both cluster DFT and periodic cell EHTB methods. Bond order calculations show that Zn preference for the Ca2 vacancy, near the OH channel and with greater structural flexibility, is associated with the formation of a four-fold (bulk) and nearly four-fold (surface) coordination, as in ZnO. When occupying the octahedral Ca1 vacancy, Zn remains six-fold in the bulk, but coordination decreases to five-fold in the surface. In the bulk and surface, Zn2 is found to be more covalent than Zn1, due to a decrease in bond lengths at the four-fold site, which approach the 1.99 Å ZnO value. Zn is however considerably less bound in the biomaterial than in the oxide, where calculated bond orders are twice as large as in HA. Surface phosphate groups (PO_4) and hydroxide ions behave as compact individual units as in the bulk; no evidence is found for the presence of HPO_4. Ca–O bond orders decrease at the surface, with a consequent increase in ionicity. Comparison between DFT and EHTB results show that the latter method gives a good qualitative account of charge and bonding in these systems.

(Some figures in this article are in colour only in the electronic version)

1. Introduction

Hydroxyapatite (HA), $Ca_{10}(PO_4)_6$ $(OH)_2$, is the ideal prototype for the basic mineral component of hard tissues such as bone and teeth. Due to its remarkable biocompatibility and osteoconductive activity, synthetic HA has been widely investigated and used as a bone repairing material for over 30 years. However, as other calcium phosphates, HA is devoid of osteoinductive properties, which expresses the desired ability of the material to induce new bone formation. As discussed in the literature [1], osteoinductive activity can be introduced by creating a 'hybrid material' in which the HA surface is chemically modified by growth factors or adsorption of adhesion proteins such as the amino acid sequence Arg–Gly–Asp (RGD), which have shown their efficacy in promoting osteoblast adhesion.

Furthermore, it is known that biological hydroxyapatite is nonstoichiometric because of the calcium deficiencies and/or the presence of a variety of trace elements such as cations (Mg^{2+}, Zn^{2+}, Sr^{2+}, Na^{+}) and anions (HPO_4^{2-}, CO_3^{2-}). These ionic losses and substitutions induce structural disorder within the HA lattice which can alter its physico-chemical properties by either causing or inhibiting normal functions. Webster *et al* [2] demonstrated enhanced osteoblast adhesion

and differentiation on HA doped with Zn, In, Bi and Y. Numerous investigations have confirmed that zinc improves the bioactivity of Zn-doped HA [3]. Recently, Capuccini *et al* [4] reported that Sr substituted for Ca into HA nanocrystals within a range of 3–7 at.% stimulated osteoblast activity and differentiation.

Zinc is one of the most important trace ions necessary for the proper function of over 80 different enzymes [5]. Several of these enzymes are involved in bone metabolism; bone is the main reservoir of zinc, which accounts for 28% of total body zinc. Zn stimulates osteoblast activity [6], collagen synthesis and alkaline phosphatase activity, which play an important role in the regulation of bone deposition and resorption [7].

One of the prerequisites for developing and designing functional hybrid organic/inorganic materials for biomedical application as RGD/HA is the understanding of the interfacial interaction between the material and biological environment. In this context, theoretical investigation of Zn adsorption on the hydrated HA surface is crucial to understand the metal uptake/release and surface properties. So far, most of the studies of Zn ions in HA are related to the bulk substitution for Ca [8]. Recently, Zn-doped ((0 0 1)) surfaces of HA have been studied by Ma and Ellis using a periodic slab density functional (DF) methodology [9]. Structural relaxation and adsorption energies were determined for Zn occupation of Ca vacancies on dry and hydrated surfaces. The site preference of Zn/Ca substitution was analysed from the point of view of total energy differences, favouring the Ca2 site. However, the mechanisms by which Zn is stabilized in the different Ca sites are not yet completely understood.

In the present work, the electronic structure of Zn substituted bulk and (0 0 1) hydrated HA surfaces are investigated and properties such as atomic charge and bonding distribution after Zn substitution at both Ca1 and Ca2 sites are calculated. A combined first principles DFT and EH tight binding [10] approach is used in which bulk and surface models are relaxed through the periodic first principles DF methodology [9]. A comparison is made between EHTB and first principles density functional calculations of the Zn1HA and Zn2HA electronic structure. This comparison validates the EHTB methodology, which is then used in calculations carried out in the surface. EHTB has already been used in different apatite systems, which showed good agreement with DFT calculations, especially concerning trends towards geometrical/site changes [11]. The early work of de Leeuw *et al* [12] and Zhan *et al* [13] on hydroxyapatite surfaces showed the importance of having computationally efficient approximate methods for geometry optimization and molecular mechanics in large systems, where first principles methods may become excessively time consuming. The present theoretical approach, which combines the computationally efficient tight binding approximation with first principles methods, points to an alternative way of using the one electron EH theory in the study of electronic properties.

Our results show that stabilization of Zn substituted hydroxyapatite, both in bulk and hydrated (0 0 1) surfaces, is related to the ability of the Ca vacancy sites to allow the formation of four-fold coordination, as in zinc oxide. This provides a simple explanation of the Zn preference for the Ca2 vacancy, near the OH channel. Calculated bond orders show four-fold (bulk) and nearly four-fold (surface) coordination for Zn2 and five- and six-fold for Zn1 (surface and bulk). Comparison between calculated bond orders in HA and ZnO shows that in the oxide they are twice as large. This indicates that, independently of position, Zn forms weaker covalent bonds in hydroxyapatite. Ca–O bonds are more ionic at the slab surfaces and do not change appreciably near substituted Zn. PO_4 and OH remain compact in the surface and calculations confirm the absence of stable HPO_4 groups near water molecules. Comparison with DFT shows that EHTB could be thought of as a convenient tool for qualitative understanding of bonding in these systems.

2. Theoretical methodology

2.1. Periodic DFT calculations

First principles structure optimizations were carried out in $2 \times 1 \times 1$ hydroxyapatite supercells $Zn_{x/y}Ca1_{8-x}Ca2_{12-y}(PO_4)_{12}(OH)_4$ $(x/y = 0, 1)$ of the Zn substituted for Ca at sites 1 and 2, on the basis of DFT theory with the Vienna simulation package VASP [14]. The relevant calculation details are: (i) the projector-augmented wave potential and a plane-wave basis set were employed, using the generalized gradient approximation (PAW-GGA) to describe exchange correlation; (ii) numerical integrations over the Brillouin zone were performed using Monkhorst–Pack K-point grids for relaxation of both bulk structures and for the calculation of total energy; (iii) the atomic positions were optimized by conjugate gradient and quasi-Newton algorithms until energy differences less than 0.02 eV/cell were obtained; (iv) Gaussian smearing was used for relaxation of ionic coordinates. In the calculations, all atomic positions were allowed to relax in both supercells, while the cell parameters were held fixed to the experimental values [15] for pure HA. K-point grids of size $2 \times 2 \times 2$ were found adequate for structure relaxation, while $4 \times 4 \times 4$ grids were used for final energy and density of states calculations.

The (0 0 1) HA hydrated surface is described by the $1 \times 1 \times 1$ slabs with six adsorbed water molecules, as described in [9]; they were relaxed, with a $2 \times 2 \times 1$ K-point grid, using the same optimization methodology described above.

2.2. Embedded cluster DFT calculations

Atomic properties and interatomic bonding structures are more conveniently defined within methods based on atomic orbital basis sets. Therefore, first principles electronic structure calculations were performed with the real-space linear combination of atomic orbitals (LCAO) discrete variational method (DVM) [16] based on local-density-functional (LDF) theory. A Mulliken-type atomic orbital population analysis is performed in order to obtain atomic charges and bond orders. The variational basis functions used are {3p, 3d, 4s, 4p} for Ca, {3d, 4s, 4p} for Zn {3s, 3p, 3d} for P, {2s, 2p} for O, and {1s} for H, with the deep-lying atomic orbitals represented as a 'frozen core'. The embedded cluster DF model was used,

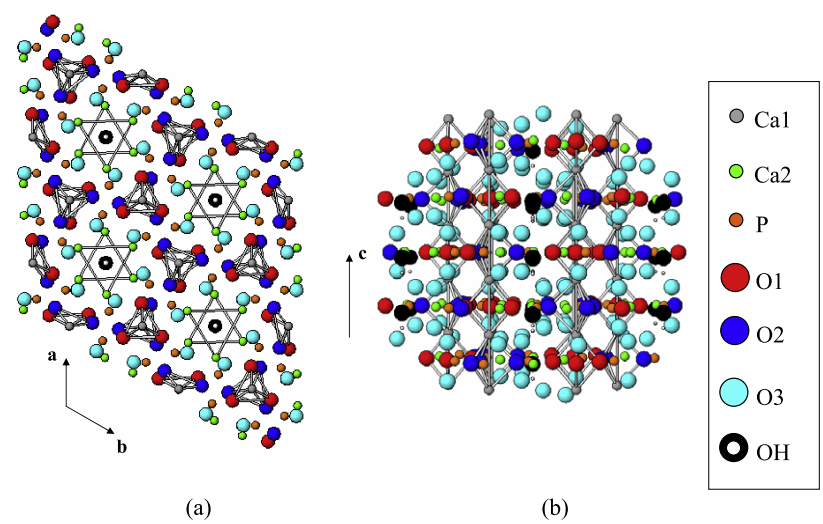

Figure 1. The unit cell of hydroxyapatite. (a) Top view; (b) side view. Note in (a) the OH channel at the centre of two Ca2 triangles and in (a) the octahedral vicinity of Ca1.

in which the surrounding atoms are included through density-derived Coulomb and exchange interactions. To investigate bonding structures at different sites, interatomic bond orders are calculated; this traditional chemical bond analysis is known to be a reliable tool to determine site preference and relative stabilities. We defined 93- and 107-atom clusters to represent, Zn1HA and Zn2HA. They were constructed from the $2 \times 1 \times 1$ supercells optimized with respect to geometry.

2.3. The EHTB method

The fundamentals of the LCAO EHTB method are well described in the literature [10]. The aspects of the theory which are relevant to the present discussion are highlighted. The basis set contains valence s and p atomic orbitals of O, P, Ca and Zn, Ca 3d, Zn 3d and H 1s, given by single (s, p) and double (d) zeta Slater functions. The empirical parameters used in the calculations are given in the appendix.

Convergence of calculated atomic charge and bond orders with the reciprocal lattice K-points set was studied in the $2 \times 1 \times 1$ Zn1 substituted supercell. By considering up to 270 k-point sets, equally distributed in the BZ, and a 12 Monkhorst–Pack set, good convergence for charge and bond orders (b.o.) was found for the latter set within 10^{-3} relative precision. All 3D calculations were performed by using the 12 points Monkhorst–Pack set. For the surface slabs a set of 18 equally distributed K-points was found to satisfy convergence of charge and b.o. EHTB calculations were performed with the BIND [17] program and the graphics were drawn with VIEWKEL [18], distributed as part of the YAeHMOP package. The program allows calculations to be done on 1D, 2D, 3D and molecular systems. In the present work we performed periodic cell 3D, 2D (EHTB) and molecular (EHMO) calculations.

In both DFT and EHTB methods, as in most LCAO approximation methods, bond orders (b.o.) between any two atoms A and B are defined by the integration, up to the Fermi level, of properly projected non-diagonal densities of states, which represent the amount of charge located in the interatomic region. They provide an estimate of the strength of the A–B bond. Higher bond orders can be associated with stronger covalent bonds. Since the basis sets used and the projection methods differ from one methodology to another, bond orders, like atomic populations, must be interpreted comparatively. In general, trends are reproduced from one method to another, giving greater confidence in the resulting models.

3. Results

3.1. Zn substitution in hydroxyapatite

We first examine charge and bond order structures of bulk HA with Zn substitution at two Ca sites and establish a comparison between EH and first principles DF cluster results. Figure 1 shows the HA structure seen in top (**a b** plane) and side (along **c**) views.

As calculations are done on Zn1-centred 93-atom and Zn2-centred 107-atom clusters, the molecular extended Hückel theory (EHMO) is used. All Ca, O and P neighbours of the central Zn atom are included in the clusters and are well coordinated with oxygen. A comparison between cluster (EHMO) and periodic cell (EHTB) calculation is given at the end of this section.

Results obtained for Zn1HA are given in table 1. Calculated atomic charges are seen to be qualitatively well described by EHMO when compared with DFT. The same trends are observed among different atom types and/or different sites for a given atom, with $q(\mathrm{P}) > q(\mathrm{Zn1}) > q(\mathrm{Ca1}) > q(\mathrm{Ca2})$ in both cases; for oxygen, one gets $q(\mathrm{O3})$ less negative than $q(\mathrm{O2})$, which is approximately equal to $q(\mathrm{O1})$. Larger differences between EH and DF calculations are found for $q(\mathrm{O4})$ and $q(\mathrm{H})$, but the net hydroxide ion charge, $q(\mathrm{OH})$, is consistently described by both methods, being -0.72 for EHMO and -0.86 for DVM. The stronger cation–anion charge transfer observed in DF cluster calculations is probably due to the weighted contribution of

Table 1. Calculated charge and bond orders in Zn1 substituted hydroxyapatite; 93-atom cluster. Atomic units.

	EHT	DVM
Charge		
Zn 1	1.700	1.989
Ca1	1.648	1.863
Ca2	1.594	1.848
P	2.604	3.244
O1	−1.263	−1.511
O2	−1.268	−1.512
O3	−1.235	−1.481
O4	−1.125	−1.607
H	0.410	0.752
OH	−0.715	−0.855
PO_4	−2.397	−2.740
Bond order		
Zn1–Ca1	0.005	−0.003
Zn1–Ca2	−0.001	0.001
Zn1–P	−0.002	−0.01
Zn1–O1	0.037	0.021
Zn1–O2	0.049	0.053
Zn1–O3 (58–60)	−0.000	−0.017

the interatomic electron density at each atom in the Mulliken-like analysis rather than on different approximations of the methods. The DF cluster uses a diagonal-weighted atomic population according to the coefficients of the wavefunction, which enhances cation–anion polarization [19]. The net charge of the PO_4 tetrahedral unit is found to be $-2.40e$ (EH) and $-2.74e$ (DF).

Bond orders involving larger interatomic distances (Zn–Ca, Zn–P, Zn–O3) are very small or negative, as expected (see table 1). In this case, comparison between the methods becomes meaningless. A better comparison can, however be done, by using nearest atom pairs, Zn1–O1 and Zn1–O2, where bond orders have larger values. In these cases EHMO is seen to reproduce DFT results fairly well, by showing the same trend among the pairs. Larger variations in the b.o. of Zn with O1 and O2 is found in DFT calculations but EHMO data fall in the range of DFT results. We have calculated EHMO orbital resolved bond orders and have found that Zn 4s and 4p interactions with O 2p orbitals contribute about 80% to the total bond order of the pair having negligible contribution from Zn 3d. This is due to the short range of d orbitals and to the fact that Zn 3d is fully occupied in the apatite system. Zn1–O1, –O2 and –O3 pair resolved bond orders were found to vary from 0.030 and 0.052, and showed six-fold coordination for Zn1, similar to Ca in site 1.

For Zn2 substituted HA we found $q(\mathrm{Zn2}) \cong q(\mathrm{Ca1}) > q(\mathrm{Ca2})$ for both EH and DF calculations. The atomic charge of Zn is smaller in site 2, having the values $q(\mathrm{Zn2}) = 1.603e$ (EH) and 1.964e (DF). Zn2–O bond orders, on the other hand, increase in comparison with site 1; we found, with EH(DF) methods, 0.085(0.029) for the pair Zn2–O2, 0.079(0.052) for Zn2–O3 and 0.11(0.034) for Zn2–O4, with total b.o. of 0.353(0.167). EH bond orders are systematically higher, but comparison between sites 1 and 2 shows good agreement with DF. This is seen from the evaluation of the relative difference between Zn1 and Zn2 total bond orders, $[\mathrm{bo(Zn2)} - \mathrm{bo\ Zn1/av.bo}] \times 100$, which was found to have the same value, 30%, within both EH and DF methods, showing consistently Zn2 as the preferred substitution site.

Zn2 clearly forms four-fold coordination in bulk HA, as the b.o. of next neighbour O pairs are considerably smaller, 0.001 and 0.0002, reproducing the coordination found in pure zinc oxide, ZnO. Therefore site 2, at the edge of the OH channel, gives more freedom for atomic rearrangements than site 1, where Zn is six-fold, so as to allow Zn2 to partly attain the oxide environment. However, the strength of Zn–O binding is not completely recovered in HA. EHTB calculation in ZnO gives a total b.o. of 0.552 while the HA result is 0.350, the two values being well correlated with the interatomic distances of 0.199 Å in ZnO and 2.052 Å (average) in HA.

The above results indicate that a reliable qualitative account of the electronic structure of Zn in hydroxyapatite can be given by the EH method, especially concerning trends towards site geometry, which is the main focus of the present study.

It remained to be determined whether the EHMO results above, which were obtained with finite cluster models, could be successfully extended to periodic cell calculations. To this aim, EHTB calculations have been performed on the periodic $2 \times 1 \times 1$ supercell. The same trend and good quantitative agreement was found within both physical models. For the most central atoms of the cluster, Zn1 and first shell Ca1, atomic charges agree with bulk calculated results within (0.7%). Other first shell atoms and groups—Ca2(2%), P(2%), O1(0.5%), O2(0.7%), O3(0.1%), OH(1%) and PO_4(1%)—also show good agreement between cluster and extended models. Next shell atomic charges are reproduced within 3%. The comparison of bond orders is even more favourable, showing differences below 10^{-4} for the next neighbour pairs. Similar results are found for Zn2HA. Therefore, the conclusions obtained above remain valid for calculations done in the periodic extended structures, which is the subject of the following analysis.

3.2. Zn1 and Zn2 on HAP001 surface

In this section we present the results of EHTB calculations carried out on the (0 0 1) hydrated model surfaces with Zn substitution on Ca1 (Zn1) and Ca2 (Zn2) sites. Figure 2 shows the unit cell for Zn substituted for Ca1 at the (0 0 1) hydrated HA slab, from side and top views, highlighting relevant bonds. Zn1 at the hydrated edge of the slab is shown connected to 1 O2, 2 O3 and 2 Ow (water oxygen) with bond lengths of 2.369 Å (O2), 2.420 Å (O3), 2.041 Å (O3), 2.166 Å (Ow) and 2.323 Å (Ow). The bond orders of each Zn1–O pair are respectively 0.017 (O2), 0.017 (O3), 0.090 (O3), 0.064 (Ow) and 0.029 (Ow). There are two remaining O2 atoms near Zn1 with bond lengths of 2.478 Å/2.731 Å and b.o. of 0.005/0.002, significantly smaller than the other five pairs. These results show a tendency of Zn1 to form five-fold coordination in the surface with the participation of two water molecules. Defining the deviation from n-fold coordination by $\Delta = \frac{\text{b.o. (total)} - \text{b.o.}(n\text{fold})}{\text{b.o.}(n\text{fold})} \times 100$ one gets $\Delta_{\mathrm{Zn1}} = 3\%$, where

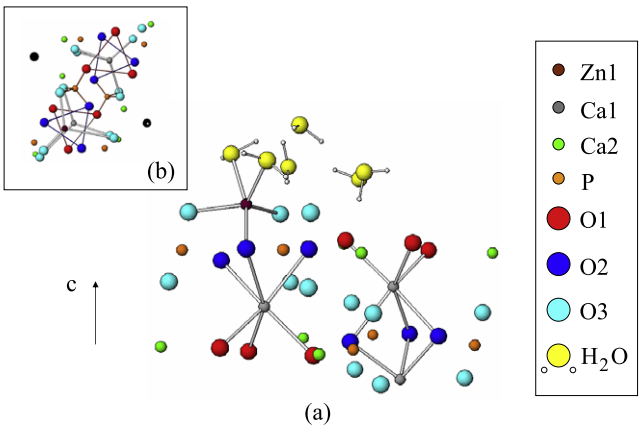

Figure 2. The unit cell of the relaxed (0 0 1) hydrated HA slab with Zn substituted at the Ca1 site. (a) Side view; (b) top view.

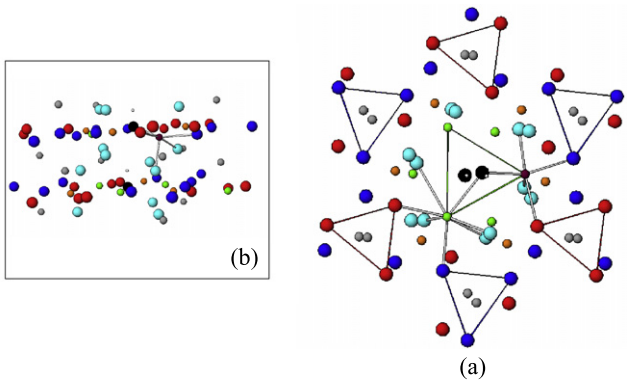

Figure 3. The unit cell of the relaxed (0 0 1) hydrated HA slab with Zn substituted for Ca2. (a) Top view; (b) side view, highlighting Zn2 coordination.

total b.o. includes bond orders larger than 0.001. In figure 2 the geometry of the five-fold coordination of Zn1 is shown.

Total Zn1–O bond order is 0.225, smaller than that described above for Zn1 in bulk HA, 0.259. The five-fold coordination of Zn1 in the HA surface is intermediate between the four-fold coordination in zinc oxide, ZnO, and the six-fold coordination of Zn1 in bulk HA. A 7% shrinkage is observed at the Zn1/(0 0 1) site, with an average bond length of 2.26 Å, when compared with the symmetrical Ca1 (in the opposite edge) with an average bond length of 2.43 Å.

In figure 3, the unit cell of a relaxed (0 0 1) hydrated slab with Zn substituted for Ca2 is seen from side and top views. Some O1 and O2 triangles around Ca1 are shown for a better understanding of the structure. One of the Ca2 belonging to the same Zn2 OH channel is shown with its oxygen bonds. By examining individual bond orders of Zn2–O pairs it is noticed that Zn2 also forms five-fold coordination at the hydrated HA surface, with b.o. varying between 0.014 and 0.118 but with a smaller deviation $\Delta = 1\%$.

Clearly, there is a tendency of Zn2 at the surface to form four-fold coordination. This could be seen from the Zn2–O1 b.o. (0.014), which is significantly smaller than the average b.o. of the remaining four pairs, of 0.070, leading to a deviation $\Delta = 6\%$. A shrinkage of 12% is found at the Zn2 site (2.186 Å) when compared with the equivalent Ca2 site (2.471 Å) (see figure 3). Other Ca2 sites in the slab have similar bond lengths, varying between 2.386 and 2.500 Å. These results indicate the greater structural flexibility of site 2. However, in the surface sites 1 and 2 they are not as distinct as they are in bulk HA, where six-fold (Zn1) and four-fold (Zn1) are more clearly defined, with deviations of 0% and 0.3%, respectively.

Table 2. Structure data, atomic charge and bonding in Zn substituted at several hydroxyapatite systems. Comparison between bulk and hydrated (0 0 1) surfaces.

Physical system	Zn1/(0 0 1)	Zn1/bulk	Zn2/ (0 0 1)	Zn2/bulk
Zn coordination	Zn1 Five-fold	Zn1 Six-fold	Zn2 Five-fold (∼ four-fold)	Zn2 Four-fold
Δ	3%	0	1%	0.3%
Total b.o.	0.225	0.259	0.298	0.350
Av. bond length	2.264	2.204	2.186	2.052
q(Zn)	1.731	1.700	1.657	1.603

We found similarities between hydrated and unhydrated (0 0 1) HA surfaces [9]: site 1 shows more uniformity in the shrinkage of Zn–O individual pairs than site 2 and, in both dry and wet slabs, a considerable shift from Zn2 towards OH and one O3 is found, with bond lengths equal to 2.073 Å/1.995 Å (dry) and 2.065 Å/1.981 Å (wet).

In table 2, a comparison is made between Zn/HA and hydrated Zn/(0 0 1). Good *bond order–bond length* correlation is found in the series, with b.o. (Zn1/(0 0 1)) < b.o. (Zn1/bulk) < b.o. (Zn2/(0 0 1)) < b.o. (Zn2/bulk) and average bond lengths decreasing in the same order. Atomic charges are also well correlated with b.o., with q(Zn1/(0 0 1)) > q(Zn1/bulk) > q(Zn2/(0 0 1)) > q(Zn2/bulk). These results point to Zn2 as being more covalent than Zn1, at both bulk and (0 0 1) hydrated slabs. The result of [9], that q(Zn2) > q(Zn1) in unhydrated slabs, can be interpreted as a result of the reduced metal coordination (five-fold and three-fold, respectively) of the dry surface.

As an estimate of Zn site preference at the hydrated (0 0 1) slabs we have obtained 28% relative b.o. difference between the two sites, favouring Zn2; this value could be compared with the bulk value of 30% found above. It is interesting to note that the relative difference between the adsorption energies of Zn on the hydrated (0 0 1) slabs, of 3.4% [9], is considerably smaller. This is due to the effects of surface relaxation around the vacancy upon removal of Zn, which is not taken into account in the b.o. estimates. The fact that bond orders follow the same behaviour as the adsorption energy indicates that local Zn–O interactions are still a main factor in Zn stabilization and could be used as a measure of Zn site preference.

Ca atoms can be classified as external and internal, according to their position in the edges of the slabs or at the central planes. Internal Ca1 total b.o. have been found to stay in range 0.55–0.58 in Zn1/(0 0 1) and 0.53–0.56 in Zn2/(0 0 1), being directly related to the average bond lengths. External Ca1, not bound to water molecules, have b.o. of 0.42 in both Zn1 and Zn2 slabs and are not geometrically correlated with internal Ca1. External Ca1 bound to water molecules show a slightly increased b.o. of 0.47 (in Zn2/(0 0 1)). Ca2 have larger

bond orders in both systems, varying from 0.66 to 0.70 in Zn1 and from 0.65 to 0.70 in Zn2 slabs, being well correlated with average bond lengths. H_2O-bound Ca2 have slightly higher bond orders than water unbound Ca2, of 0.75 (in Zn1/(0 0 1)) and 0.74 (in Zn2/(0 0 1)). Both Ca1 and Ca2 connected directly to water are seven-fold coordinated.

There is a clear surface effect, which can be observed above from the decrease in the bond orders of Ca1 located at the external faces. Atomic charges also give evidence of surface formation. For the Zn1/(0 0 1) slab we have obtained external q(Ca1) = 1.74 greater than the internal Ca1 charges, of 1.61 and 1.64. For Zn2/(0 0 1), external q(Ca1) = 1.67 (water-bound) and 1.74 (water unbound); while internal q(Ca1) were found to be 1.63 and 1.64. Conversely, oxygen charges tend to be more negative near the exposed faces of the slabs. In the Zn1/(0 0 1) slab we have obtained q(O) in the range −1.29 to −1.33 for external O3 atoms, and −1.22 to −1.27 for O atoms more internal. In Zn2/(0 0 1), external O3 atoms have atomic charges between −1.30 and −1.32 and for the internal atoms the values range between −1.22 and −1.30. In both system slabs, external faces are more polarized, a result which has also been found in HA unhydrated (0 0 1) surfaces [20].

We have investigated more closely the interaction of hydrogen atoms of water molecules, Hw, with phosphate groups. It has already been pointed out that hydration of HA (0 0 1) surfaces apparently does not cause the formation of HPO_4 [9]. In fact, this is confirmed in the present calculations of Hw–O bond orders. There are three O3 slab oxygen atoms near the hydrated face and two of them form larger bonds with Hw but still too small when compared with the P–O b.o. For Zn1/(0 0 1), Hw–O3 b.o. are 0.06 and 0.04 while in the corresponding phosphate group individual b.o. are in the range 0.67–0.68. In Zn2/(0 0 1), Hw–O3 b.o. are 0.05 and 0.06 and there is an additional Hw–O1 pair with b.o. equal to 0.03, while the P–O range from 0.67 to 0.68. All phosphate groups behave as strongly covalent compact units, independent of their relative positions in the slabs.

Average O–H bond orders of HA hydroxy ions (0.60) are similar to those of Ow–Hw (varying from 0.55 to 0.59) in both Zn1/(0 0 1) and Zn2/(0 0 1) slabs. It is found that any two neighbouring water molecules form weak H–O bonds with b.o. of 0.04, one order smaller than those found in intra-H_2O pairs.

4. Conclusion

We have used a combined DFT–EHTB theoretical approach to study atomic scale interactions in Zn substituted bulk and hydrated (0 0 1) hydroxyapatite surfaces. Periodic DFT calculations were done for geometry optimization of Zn1 and Zn2 substituted bulk HA. Molecular cluster DFT and EHTB calculations were also performed in these systems. The EHTB method provided a reliable account of charge and bond order structures, predicting the Zn preference for Ca2 sites in qualitative and quantitative agreement with DFT results. While quantitatively different, calculated atomic charges and bond orders follow the same trend among different atom types and crystal positions for either method. DVM charge distribution shows higher cation–anion charge transfer than EH calculations; differences between the methods have an average of about 15%. The EHTB method was then used in the study of Zn1 and Zn2 substituted hydrated (0 0 1) HA slabs.

As a main result, the present calculations have shown Zn preference for substitution at Ca2 sites in bulk and hydrated (0 0 1) HA surfaces, in accordance with previous total energy calculations for (0 0 1) HA surfaces. The Ca2 vacancy site, near the OH channel, has more structural flexibility, thus allowing Zn to form four-fold (bulk) and almost four-fold (surface) coordination, as in ZnO, with more than 10% shrinkage of the average bond length when compared with symmetrical Ca2 sites. When substituting for Ca1, Zn forms six-fold (bulk) and five-fold (surface) coordination with an average bond length similar to that of Ca. Zn2 is found to have stronger covalent character than Zn1. It is found that both Zn1 and Zn2 in HA are less covalent than in zinc oxide, where the bond orders are twice as high, showing Zn to be loosely bound in hydroxyapatite. Zn1–O and Zn2–O bond orders in HA (bulk and surface) are well correlated with the average Zn–O distance in each site. From this it could be seen that, although Zn1 forms bonds with adsorbed water molecules, no net increase in bond order is found due to hydration.

Other results of the present study are: (i) cation and anion charges are increased at the external faces of the surface slabs, which exhibit higher electric polarization than the bulk; (ii) PO_4, OH and H_2O remain compact as in bulk HA; (iii) although a small H–O bond was detected between water molecules and phosphate, no effect was observed in the charge and bond orders of the phosphate, with no evidence of HPO_4 formation in the hydrated surface; (iv) the effect of Zn substitution is mainly local, as no significant charge and Ca–O bond order perturbation was found near Zn sites; (v) non-negligible inter-molecular O–H bond orders were found among the H_2O molecules in the 1.6 Å-wide water layer, which has been found in the literature to present low mobility.

Acknowledgments

The work of DEE was supported in part by the US Dept. of Energy, BES, through the Northwestern University Institute of Catalysis in Energy Processes.

Appendix

Table A.1 shows the EH parameters used in the calculations. For Ca 4s and 4p, P, O and H the parameters were taken

Table A.1. Atomic eHT parameters. n: principal quantum number; energies in eV.

	n	$h_{ns,ns}$	ξ_{ns}	$h_{np,np}$	ξ_{np}
Ca[4]	4	−6.111	1.2	−4.219	1.2
Zn	4	−10.55	2.65	−6.30	2.65
O[8]	2	−32.3	2.575	−14.8	2.275
P[9]	3	−18.6	1.75	−14.0	1.30
H[8]	1	−13.6	1.3	—	—
Ca 3d: $h_{3d,3d} = -6.185$; $c_1/c_2 = 0.400/0.700$; $\xi_1/\xi_2 = 4.0/1.300$					
Zn 3d: $h_{3d,3d} = -22.302$; $c_1/c_2 = 0.590/0.570$; $\xi_1/\xi_2 = 6.15/2.60$					

from [11]. Bochmann *et al* [21] used a similar set of Zn parameters in a study of ZnS_3 complexes. To describe oxygen zinc interactions, we have made a scale transformation based on bond lengths to the exponents of the 4s and 4p basis functions [22] and Zn 3d was adjusted to reproduce the band structure of zinc oxide, whose Zn 3d–O 2p separation of 7.5 eV is known from experiment [23].

References

[1] See for example, LeGeros R Z 2008 *Chem. Rev.* **108** 4742–53
Anselme K 2000 *Biomaterials* **21** 667–81

[2] Webster T J, Ergun C, Doremus R H and Bizios R 2002 *J. Biomed. Mater. Res.* **59** 312–7
Webster T J *et al* 2004 *Biomaterials* **25** 2111–21

[3] Grandjean-Laquerriere A, Laquerriere P, Jallot E, Nedelec J M, Guenounou M and Laurent-Maquin D 2006 *Biomaterials* **27** 3195
Jallot E, Nedelec J M, Grimault A S, Chassot E, Grandjean-Laquerriere A, Laquerriere P and Laurent-Maquin D 2005 *Colloids Surf.* B **42** 205
Fujii E, Ohkubo M, Tsuru K, Hayakawa S, Osaka A, Kawabata K, Bonhomme C and Babonneau F 2006 *Acta Biomater.* **2** 69

[4] Capuccini C, Torricelli P, Boanini E, Gazzano M, Giardino R and Bigi A 2009 *J. Biomed. Mater. Res.* A **89** 594–600

[5] Peretz A, Papadopoulos T, Wiltems D, Hotimsky A, Michiels N, Siderova M, Bergmann P and Neve J 2001 *J. Trace Elem. Med. Biol.* **15** 175–8

[6] Kawamura H, Ito A, Miyakawa S, Layrolle P, Ojima K, Ichinose N and Tateishi T 2000 *J. Biomed. Mater. Res.* **50** 184–90
Brandao-Neto J, Stefan V, Mendonca B B B, Blois W and Castro A V 1995 *Nutr. Res.* **15** 335–58

[7] Yamaguchi M and Yamaguchi R 1986 *Biochem. Pharmacol.* **35** 773–7
Yamaauchi M, Oishi H and Suketa Y 1987 *Biochem. Pharmacol.* **36** 4007–12

[8] Terra J, Jiang M and Ellis D E 2002 *Phil. Mag.* A **77** 2357–77
Matsunaga K 2008 *J. Chem. Phys.* **128** 245101
Tang Y, Chappel H F, Dove M T, Reeder R J and Lee Y J 2009 *Biomaterials* **30** 2864–72

[9] Ma X and Ellis D E 2008 *Biomaterials* **29** 257–65

[10] Hoffmann R 1963 *J. Chem. Phys.* **39** 1397
Summerville R H and Hoffmann R 1976 *J. Am. Chem. Soc.* **98** 7240
Hoffmann R 1989 *Solids and Surfaces* (New York: Wiley-VCH)

[11] Matos M, Terra J and Ellis D E 2009 *Int. J. Quantum Chem.* **109** 849–60

[12] Mkhonto D and De Leeuw N H 2002 *J. Mater. Chem.* **12** 2633–42
De Leeuw N H 2004 *Phys. Chem. Chem. Phys.* **6** 1860–6

[13] Zahn D and Hochrein O 2003 *Phys. Chem. Chem. Phys.* **5** 4004–7

[14] Kresse G and Hafner J 1993 *Phys. Rev.* B **47** 558–61
Kresse G and Furthmüller J 1996 *Phys. Rev.* B **54** 11169–86
Kresse G and Furthmüller J 1996 *Comput. Mater. Sci.* **6** 15–50

[15] Kay M I, Young R A and Posner A S 1964 *Nature* **204** 1050–2

[16] Ellis D E and Painter G S 1970 *Phys. Rev.* B **2** 2887
Rosen A and Ellis D E 1975 *J. Chem. Phys.* **62** 3039
Ellis D E and Guenzburger D 1999 *Adv. Quantum Chem.* **34** 51
Ellis D E and Guo J 1995 *Electronic Density Functional Theory of Molecules, Clusters, and Solids* ed D E Ellis (Dordrecht: Kluwer) p 263
Ellis D E 1985 *Handbook on the Physics and Chemistry of the Actinides* ed A J Freeman and G H Lander (Amsterdam: North-Holland) p 1. (The DVM academic program has its evolved commercial counterparts in the ADF (Amsterdam density functional) and DMOL packages)

[17] Landrum G A and Glassey W V 2001 *bind (ver 3.0)* bind is distributed as part of the YAeHMOP extended Hückel molecular orbital package and is freely available on the www at: http://sourceforge.net/projects/yaehmop

[18] Landrum G A 2001 *viewkel (ver 3.0)* viewkel is distributed as part of the YAeHMOP extended Hückel molecular orbital package and is freely available on the www at: http://sourceforge.net/projects/yaehmop

[19] Schramm D U, Terra J, Rossi A M and Ellis D E 2000 *Phys. Rev.* B **63** 024107

[20] Rulis P, Yao H, Ouyang L and Ching W Y 2007 *Phys. Rev.* B **76** 245410

[21] Bochmann M, Bwembya G, Grinter R, Lu J, Webb K J, Williamson D J, Hursthouse M B and Mazid M 1993 *Inorg. Chem.* **32** 532–7

[22] Matos M 1999 *J. Mol. Struct. (Theochem)* **464** 129–35

[23] Özgür Ü, Alivov Ya I, Liu C, Teke A, Reschikov M A, Dogan S, Avrutin V, Cho S-J and Morkoç H 2005 *J. Appl. Phys.* **98** 041301